Journal of Data Acquisition and Processing
ISSN: 1004-9037
https://sjcjycl.cn/
DOI: 10.5281/zenodo.777935

ACTIVE, REACTIVE POWER COMPENSATION AND DYNAMIC RESPONSE OF SEIG WTGS WITH 48 PULSE STATCOM BY USING INTELLIGENT CONTROLLERS

S.Radha Krishna Reddy[1] Dr.J.B.V.Subrahmanyam[2] Dr. A. Srinivasula Reddy[3]

[1]Research Scholar, EEE Dept, JNTU Hyderabad, Hyderabad, India

[2]Professor&Principal, EEE Dept, Holy Mary Institute of Technology & Science, JNTUH, Hyderabad, India

[3]Professor&Principal, EEE Dept, CMR Engineering College, JNTUH, Hyderabad, India

[1]rkphd2012@gmail.com, [2]jbvsjnm@gmail.com, [3]svas_a@yahoo.com

ABSTRACT: Wind Turbine Generator systems (WTGs) have become one of the most popular renewable energy sources in many nations because of their low costs, low maintenance, and great operational reliability. With the Grid-connected WTG, power, frequency, and voltage are synchronized. In wind farms, reactive power compensation devices like STATCOM are employed. Using a STATCOM, the source and load voltages can be kept stable, while improving the power quality, while a series voltage is injected between them. We build a dynamic model of SEIG–STATCOM that feeds nonlinear loads through the use of WTG and STATCOM operating in concert with vector control based on phase-locked loops (PLL), in order to anticipate how the system will behave in transient scenarios. The dynamic responsiveness of the WTG and harmonic elimination are provided by a three-phase 48 pulse inverter working as a STATCOM to provide the reactive power required by SEIG in order to maintain a consistent terminal voltage with changing wind speed input and loads. Voltage and power quality were improved by using an artificial neural network (ANN) on a self-excited induction generator with a constant speed prime mover connected to the grid (Artificial Neural Network). An ANN-based control method was designed for WTG and STATCOM in the event of a malfunction. The MatLab software is used to mimic the PI Fuzzy and ANN controllers' performance. Maintaining synchronicity is done by balancing the active powers at both ends. When the voltage profile is out of whack, the ANN controller maintains a stable voltage profile by sending reactive power to the WTG through STATCOM.

Keywords: Artificial Neural Network(ANN),Self-Excited Induction Generator, STATCOM (Static Compensator),Phase-Locked Loops (PLL).

I. Introduction

Renewable energy investment has thrived in rural regions that have been electrified. Due to their lower costs, off-grid distant places make substantial use of renewable energy sources like wind and solar power, biogas, hydropower, and other hydroelectric types [1,2]. SEIGs are among the most efficient generators to run on their own because of their many advantages, such as low maintenance costs, mechanical simplicity, and robust construction [3,4]. Externally driven induction machine (SEIG) excitation requirements are fulfilled by a capacitor bank linked to the machine's terminals. Because it lacks DC and is brushless, the SEIG is an excellent alternative to a traditional synchronous generator. Documentation of SEIG steady-state and transient analysis in the literature is extensive. SEIG's transient research [1]–[3] makes use of a dq axis model. Using an imbalanced excitation system, Wang and Deng [4] demonstrated the SEIG's transient performance. SEIG transient analysis under symmetrical and non-symmetrical situations has been analyzed by Jain et al. [5]. There has been a rise in the use of power electronic converters for standalone applications due to an increase in the emphasis on renewable electric energy generation. A variety of network operating conditions can be accommodated by SEIG's dynamic analysis. As the speed of the wind changes, the induction generator used in wind energy conversion systems must adjust its rotating speed accordingly. Saturated self-excited induction generators for renewable energy generation were modelled using the d-q theory. The machine must be magnetized by an external reactive supply in order to be used as an autonomous generator [5]. Using the rotor residual flux and a capacitor bank coupled to the stator terminals, an induced voltage can be generated for any given wind speed [6]. However, the harmonics introduced into the isolated grid by the line current switching make both options unappealing. The usage of STATCOMs in off-grid plants has expanded due to the widespread use of rapid commutating switches, which has shown improved stability and performance in wind conversion systems [16,17]. One of the first compensators to use a voltage inverter [18] was this one. An alternative control technique is to use the SEIG terminals to create a statically compensated STATCOM compensator. By controlling the active and reactive power flow, the suggested system attempts to manage output frequency and stabilize the generated voltage. The suggested structure's general layout is shown in Fig.1. By way of a coupling

transformer, a capacitor bank-powered SEIG is connected to the STATCOM. As a whole, it supplies an electrical demand that can fluctuate. Power quality improvement using an isolated asynchronous generator (IAG) based multi-pulse electronic load controller. THD (Total Harmonic Distortion) can be calculated from the simulation data using Fast Fourier Transform (FFT) (Fast Fourier Transformation). Based on renewable energy applications in remote places, while feeding single-phase loads, the comparison of alternative terminal capacitor connections is dependent on the maximum anticipated load, voltage and frequency changes that can be tolerated, and reactive power requirements [14] to determine this load. The dynamic performance of an isolated SEIG operated by a fixed pitch wind turbine is presented in this research. Analysis and verification of SEIG performance under a variety of static load scenarios have been completed. Several researchers [13] have employed shortend long-shunt techniques for SEIGs. Regardless of the type of load, the terminal voltage cannot be kept constant with this method. Many investigations have used the static var compensator, which consists of a fixed excitation capacitor and a TCR [14]. SVC (thyristor-controlled inductor) [6] and short shunt capacitor connections [8] were used to maintain a consistent terminal voltage. Harmonics are supplied into the production system as a result of these systems' discrete voltage regulation. Using SEIG, it is now possible to design a static noiseless voltage regulator that can supply SEIG with continuously changing reactive power while retaining the terminal voltage constant. There are certain advantages of using STATCOM over SVC [9], respectively. A static VAR compensator can be used to stabilize a pumping system powered by an induction generator. SEIG voltage management under unbalanced/nonlinear load conditions is described by Kuo and Wang [14] (VSI).

Under linear, nonlinear, balanced, or unbalanced loads, STATCOM can be used to maintain a harmonic-free SEIG terminal voltage. Harmonics are reduced and the load is balanced with its help. Considering the excitation capacitances is necessary in order to arrive at a stable voltage value. The wind turbine's self-excited induction generator is used to track and collect the maximum power from the grid. Use the variable frequency and constant voltage converter to compensate for reactive power. When selecting capacitors, a variety of factors must be taken into account, including the machine's frequency, magnetic reactance, and other independent variables. System efficiency and power handling capability have been proven to be stable and regulated.

Consequently, it is very responsive to changes in parameters. In recent years, artificial neural networks (ANNs) have emerged as a cutting-edge technique for electrical system analysis. [14–17] Due to the non-linearity of the parallel design, the controller can perform faster because it does not need a precise input-output relation. Its robustness cannot be matched by a normal controller. A self-sustaining DC bus is the goal here, rather than the more usually mentioned shunt voltage controller like STATCOM. Three-phase linear and nonlinear loads may be fed by wind turbine prime movers operated by SEIG. Batteries aren't required for the proposed STATCOM, which uses a self-support DC bus and a smaller and less expensive voltage source converter (VSC). STATCOM employs STATCOM in addition to PI, Fuzzy, and ANN-based basic control systems. ANN toolkit is used to examine the ANN and PI-based STATCOM's performance in MATLAB. The power electronics device STATCOM has a DC bus in series with the SEIG and loads, a VSC-based power electronics device MATLAB is used throughout the process of developing, modelling, and simulating the entire system.

II. MATHEMATICAL ANALYSIS OF SEIG SYSTEM

The Modelling of Self-Excited Induction Generators By reducing three-axis models to just two, electrical machine analysis makes finding solutions a whole lot easier. Real-world three-phase power systems are depicted by the three axes. Assumed to be stationary in the reference frame are the three and two axes of rotation. The abc and stationary dq0 axes can be rephrased as a transformation. A steady-state induction machine can be described using an equivalent circuit. In dynamic contexts, however, the SEIG is modelled using the d-q representation. On the stator side of the SEIG, there is no electrical input from the rotor, thus capacitors are coupled to the terminals of the stator winding. Direct and quadruple stator types are shown in the following figure.

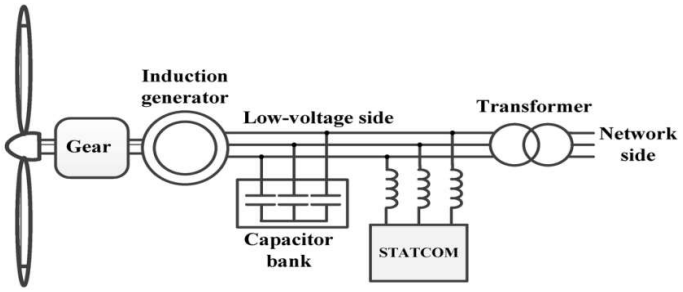

Fig.1 – SEIG powered by a wind turbine's capacitance excitation system

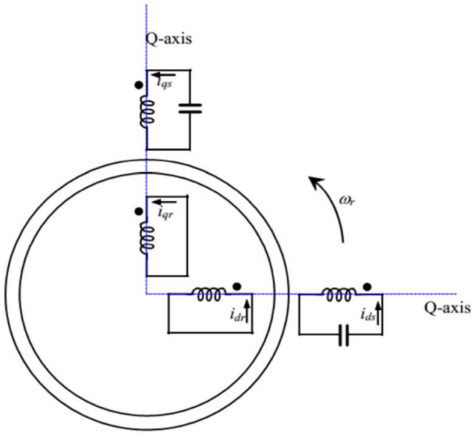

Fig.2. dq diagram of an induction generator that is self-excited

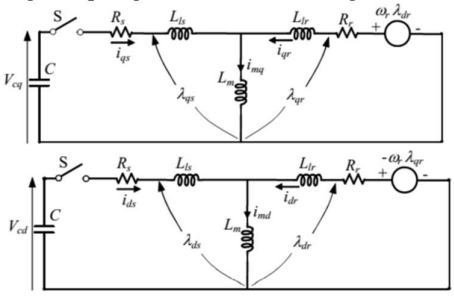

Fig.3 – dq reference frame model of SEIG circuits (a) D-axis and q-axis circuitry

The capacitor voltages in Fig. 2. can be represented as

$V_{cq} = \frac{1}{C}\int i_{qs}dt + V_{cq0}$------(1)

$V_{cq} = \frac{1}{C}\int i_{ds}dt + V_{cd0}$------(2)

Where$V_{cq0} = V_{cq}$, at t=0 and $V_{cd0} = V_{cd}0$, at t=0 is the initial voltage along with the q-axis and d-axis capacitors, respectively. The rotor flux linkage is given by

d-axis capacitors, respectively.

The rotor flux linkage is given by

$\lambda_{qr} = L_m i_{qs} + L_r i_{qr} + \lambda_{qr}$ ------(3)

$\lambda_{dr} = L_m i_{ds} + L_r i_{dr} + \lambda_{dr0}$------(4)

where

$L_s = L_{ls} + L_m$ and $L_r = L_{lr} + L_m$;------(5)

$$\lambda_{qr0} = \lambda_{qr}\ at\ t = 0, and\ \lambda_{qr0=\ qr}$$

remnant and residual rotor flux links are located at t=0, respectively, along the q-axis and the d-axis. the rotational voltage in this circuit can be expressed as qr = r/q.

$\omega_r\lambda_{qr} = \omega_r(L_m i_{qs} + L_r i_{qr}) + \omega_r K_{dr0}$------(6)

$\omega_r\lambda_{dr} = \omega_r(L_m i_{ds} + L_r i_{dr}) + \omega_r K_{qr0}$------(7)

Similarly, the rotor circuit's d axis rotational voltage is.

$\omega_r\lambda_{dr} = \omega_r(L_m i_{ds} + L_r i_{dr}) + \omega_r K_{qr0}$------(8)

$\omega_r\lambda_{qr} = \omega_r(L_m i_{qs} + L_r i_{qr}) + \omega_r K_{dr0}$------(9)

Assume that the initial voltages of the two directions are K qr0=K qr and K dr0=K dr. K dr0 and K qr0 are constant because of the core's residual magnetic flux. The equivalent electrical rotation speed in revolutions per second (r/s) is r. That's what I'm talking about.

There are a fixed number of pole pairs and the mechanical speed of each is equal to the electrical speed

Assuming the stationary stator reference frame in the d-q model of self-excited induction generator, the matrix equation:

$$\begin{bmatrix} R_s + L_s + {}^{1}/_{C} & 0 & L_m & 0 \\ 0 & R_s + L_s + {}^{1}/_{C} & 0 & L_m \\ L_m & -\omega_r L_m & R_r + L_r & -\omega_r L_m \\ \omega_r L_m & L_m & \omega_r L_m & R_r + L_r \end{bmatrix}$$

$$[Z][I_v] + [V_v] = [0]$$

Since the initial situation has an effect on the stator and rotor currents and the voltage vector, Z is the impedance matrix

Modelling of SEIG under Different Loading

When building an induction generator model in a dq reference frame, it is necessary to translate variables from three axes to two axes. These parameters are not influenced by per-phase changes in machine parameter values. Figure 4 shows an equivalent circuit model in the dq reference frame, as can be observed. Every similar circuit element in the dq reference frame has the same value for each phase of a three-phase machine.

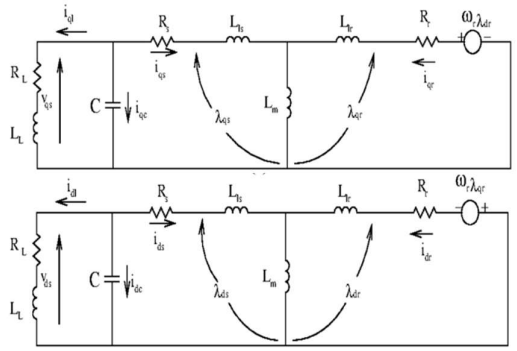

Fig.4 – dq reference frame model of SEIG circuits (a) d-axis and q-axis circuitry.

We may derive the following voltage equations from the aforementioned circuit using KVL:

$V_{qs} = R_s i_{qs} + \frac{d\lambda_{qs}}{dt}$ ------(10)

$V_{ds} = R_s i_{ds} + \frac{d\lambda_{ds}}{dt}$------(11)

$$0 = R_r i_{qr} + \frac{d\lambda_{qr}}{dt} - \omega_r \lambda_{qr}$$

$$0 = R_r i_{dr} + \frac{d\lambda_{dr}}{dt} - \omega_r \lambda_{dr}$$

Where$V_{qr}\ \ V_{dr} = 0$

Expressions for flux linkage using currents can be written.

$\lambda_{qs} = L_s i_{qs} + L_m i_{qr}$------(12)

$\lambda_{qr} = L_s i_{qr} + L_m i_{qs}$------(13)

$\lambda_{qr} = L_s i_{qr} + L_m i_{qr}$------(14)

$\lambda_{dr} = L_s i_{dr} + L_m i_{ds}$------(15)

It is possible to obtain the following differential equation from eqn.(2.11-2.15)

$\frac{di_{sq}}{dt} = \frac{1}{L_s L_r - L_m^2}[-L_s R_s i_{sq} - \omega_r L_m^2 i_{sq} + L_m R_r i_{qr} - \omega_r L_m L_r i_{rq} + L_r V_{sq}]$------(16)

$\frac{di_{sd}}{dt} = \frac{1}{L_s L_r - L_m^2}[-L_s R_s i_{sd} - \omega_r L_m^2 i_{sd} + L_m R_r i_{dr} - \omega_r L_m L_r i_{rd} + L_r V_{sd}]$------(17)

$\frac{di_{rq}}{dt} = \frac{1}{L_s L_r - L_m^2}[L_m R_s i_{sq} + \omega_r L_m^2 L_s i_{sq} - L_s R_s i_{qr} + \omega_r L_s L_r i_{dr} + L_m V_{sq}]$------(18)

$\frac{di_{rq}}{dt} = \frac{1}{L_s L_r - L_m^2}[L_m R_s i_{sq} - \omega_r L_s L_m i_{sq} - L_s R_r i_{dr} + \omega_r L_s L_r i_{qr} + L_m V_{sd}]$------(19)

Where

$$L_s = L_{ls} + L_m, L_r = L_{lr} + L_m$$

The expression for electromagnetic torque is given by

$T_e = \left(\frac{3}{2}\right)\left(\frac{P}{2}\right) L_m\left[i_{qs} i_{qr} - i_{ds} i_{dr}\right]$------(20)

The expression for magnetizing current is given as

$$i_m = \sqrt{(i_{sd} + i_{rd})^2 + \left(i_{sd} + i_{rq}\right)^2}$$

MODELING OF SEIG–STATCOM SYSTEM

In order to construct a mathematical model of the SEIG–STATCOM system, we must first model both SEIG and STATCOM.

Control Scheme Modelling for the STATCOM Figs. 1(a) and (b) demonstrate the components and control systems of the SEIG-STATCOM system; these are shown as follows. Use this formula $v_a, v_b, v_c$to get the amplitude of three-phase sinusoidal voltages at the SEIG terminals.

$V_t = \{({}^{2}/_{3})(v_a^2 + v_b^2 + v_c^2)\}^{\frac{1}{2}}$------(20)

The unit vectors in phase with v_a, v_b, v_c are derived as

$$u_a = {}^{v_a}/_{v_t}\,;\; u_b = {}^{v_b}/_{v_t}\,;\; u_c = {}^{v_c}/_{v_t}$$

A quadrature transformation of in-phase unit vectors u_a, u_b, u_c [11] can be used to generate the quadrature unit vectors with v_a, v_b, v_c.

$\omega_a = -{}^{u_b}/_{\sqrt{3}} + {}^{u_c}/_{\sqrt{3}}$ ------(21)

$\omega_b = {}^{\sqrt{3}u_a}/_{2} + {}^{(u_b - u_c)}/_{2\sqrt{3}}$ ------(22)

$\omega_c = {}^{\sqrt{3}u_a}/_{2} + {}^{(u_c - u_a)}/_{2\sqrt{3}}$ ------(23)

Reference Component with quadrature Atmospheric Winds: Inaccuracy in the ac voltage at sampling point n, the value of is

$$V_{er(n)} = V_{tref} - V_{t(n)}$$

For example, V_{tref} is the reference voltage and Vt(n) represents three-phase ac voltages sensed at SEIG terminals at that particular instant in time. At the nth sampling instant, the output of the PI controller $I^*_{smq(n)}$ is expressed as

$I^*_{smq(n)} = I^*_{smq(n-1)} + K_{pa}\{V_{er(n)} - V_{er(n-1)}\} + K_{ia}V_{er(n)}$ ------(24)

At the n-1st instant of the PI controller's gain, $V_{er(n)}$ is the voltage error, and $I^*_{smq(n-1)}$ is the amplitude of the reference source current, with K_{ia} being its constant gain. The quadrature components of the reference source currents are estimated.

$$i^*_{saq} = I^*_{sm}\ \omega_a; i^*_{sbq} = I^*_{smq}\omega_b; i^*_{scq} = I^*_{smq}\omega_c;$$

In-Phase Reference Component Atmospheric Winds: The nth sampling moment dc bus voltage error $V_{dcer(n)}$ is

$V_{dcer(n)} = V_{dcref} - V_{dc}$ ------(25)

The dc voltage reference here is V_{dcref}, while the STATCOM connection voltage is V dc(n). At sampling instant n, this is the output of the PI controller for maintaining the dc bus voltage of the STATCOM:

$I^*_{smd(n)} = I^*_{smq(n-1)} + K_{pd}\{V_{der(n)} - V_{der(n-1)}\} + K_{id}V_{der(n)}$ ------(26)

$I^*_{smd(n)}$is the amplitude of the source current's active power component. The dc bus PI voltage controller's proportional and integral gain constants are K_{pd} and Kid, respectively. Reference source currents' in-phase components are estimated.

$$i^*_{sad} = I^*_{smd}u_a; i^*_{sbd} = I^*_{smd}u_b; i^*_{scd} = I^*_{smd}u_c;$$

Referencing Source Total Current: Referencing Source Total Current is the total of reference source currents in phase and quadrature as

$i^*_{sa} = i^*_{saq} + i^*_{sad}$ ------(27)

$i^*_{sb} = i^*_{sbq} + i^*_{sbd}$ ------(28)

$i^*_{sc} = i^*_{scq} + i^*_{scd}$ ------(29)

III. Modelling of STATCOM

Current-controlled voltage stabiliser (VSI) STATCOM is modelled as follows. The following is the definition of the dc bus voltage's derivative:

$$v_{dc} = (i_{csa} + i_{csb} + i_{csc})/C_{dc}$$

In this case, the VSI bridge switches S1–S6 are controlled by the switching functions. the output of the inverter is the three-phase PWM ac line voltages, all of which are stated as

$$V_a = V_{dc(sa-sb)}$$
$$V_b = V_{dc(sb-sc)}$$
$$V_c = V_{dc(sc-sa)}$$

The voltage and current equations of VSI STATCOM are

$V_a = Ri_{ca} + Li_{ca} + e_a - Ri_{cb} - Li_{cb}$------(30)

$V_b = Ri_{cb} + Li_{cb} + e_b - Ri_{cc} - Li_{cc}$------(31)

$V_c = Ri_{cc} + Li_{cc} + e_c - Ri_{ca} - Li_{ca}$-----(32)

$i_{ca} + i_{cb} + i_{cc} = 0$ ------(33)

The value of i_{cc} from (33) is substituted into (31) which results in

$$V_b = Ri_{cb} + Li_{cb} + e_b + Ri_{ca} + Li_{ca} + Ri_{cb} + Li_{cb}$$

Modelling of SEIG

Static dq axis reference frames with voltage–current equations are used to create the dynamic model of the three-phase SEIG.

$$[V] = Ri + Li + \omega_g Gi$$

By the above equation currents can be derivatives

$$i = [L]^{-1}\{V - Ri - \omega_g Gi\}$$

where;

$$[V] = [V_{ds}V_{qs}V_{dr}V_{qr}]^T$$
$$[i] = [i_{ds}i_{qs}i_{dr}i_{qr}]^T$$
$$[R] = |[R_sR_sR_rR_r]|$$
$$L = \begin{bmatrix} L_s + L_m & 0 & L_m & 0 \\ 0 & L_s + L_m & 0 & L_m \\ L_m & 0 & L_r + L_m & 0 \\ 0 & L_m & 0 & L_r + L_m \end{bmatrix}$$
$$G = \begin{bmatrix} 0 & 0 & 0 & 0 \\ 0 & 0 & 0 & 0 \\ 0 & -L_m & 0 & L_r + L_m \\ L_m & 0 & L_r + L_m & 0 \end{bmatrix}$$
$$I_m = \sqrt{\{(i_{ds} + i_{dr})^2 + (i_{qs} + i_{qr})^2\}/\sqrt{2}}$$

The magnetising characteristic between L_m and I_m is used to compute the magnetising inductance. A synchronous speed test [11] yields a relationship between L_m and I_m that can be expressed as

$$L_m = A_1 + A_2 I_m + A_3 I_m^2 + A_3 I_m^2$$

The coefficients A1, A2, A3, and A4 are given in C.

ACTIVE REACTIVE POWER, VOLTAGE AND FREQUENCY CONTROL STRATEGIES

The voltage and frequency of the SEIG stator terminals are monitored as part of the proposed control method. The STATCOM, in reality, must interchange an active and reactive power flow with the system in response to changes in wind speed or associated loads.

Control of reactive power

When a wind turbine and system-based STATCOM are connected, the reactive power flow can be used to alter the voltage at PCC. PI controllers with GA-tuned settings are used to minimise the square error integral when the voltage at PCC changes (ISE).Diagram of the STATCOM system with two PI controllers may be shown in Figure 3. The PCC uses the three-phase signals to generate a d–q frame. There are two PI controllers that control STATCOM's many functions. The Iqref reference quadrature current is updated by using controller 1 and the vector difference between the measured and reference voltage. this. A different direction can be chosen for the PCC's terminal voltage phase angle when it is used. Controller 2 is used for this. With STATCOM's PWM technology, the voltage output of its three-level inverter system is controlled by phase angle control. Signals that are subject to manipulation:

Regulating the voltage

In order to adjust for a voltage fluctuation, the regulator PI estimates the value of the modulation index m. The input PI regulator's rms voltage error, then, is calculated as follows for a sample order of n:

$$\Delta V_{Ig.err(n)} = V^*_{Ig(n)} - V_{Ig(n)}$$

The modulation index at the controller output is calculated as follows:

$$m(n) = m(n-1) + K_{pv}[\Delta V_{Ig.err(n)} - \Delta V_{Ig.err(n-1)}] + K_{iv}\Delta V_{Ig.err(n)}$$

With, K_{pv} and $K_{iv}$are respectively regulator parameters.

Frequency regulation

Action on phase shift monitors power flow and ensures that the frequency remains stable.

The sample order n error frequency is represented as follows:

$$\Delta f_n = f *_n - f_n$$

And the output PI regulator is:

$$\delta_n = \delta_{n-1} + k_{pv}[\Delta f_n - \Delta f_{n-1}] + K_{iv}\Delta f_n$$

Therefore, the three-phase reference voltages for the PWM control of the VSI are deduced as:

$$\begin{cases} V *_a = msin(\omega t + \delta) \\ V *_b = msin(\omega t + \delta - \frac{2\pi}{3}) \\ V *_c = msin(\omega t + \delta - \frac{4\pi}{3}) \end{cases}$$

DC Link Voltage

The DC link voltage is selected from the following equation:

$$V_{dc} = \frac{\sqrt[2]{2(V/\sqrt{3})}}{mod - index}$$

in which the modulation index (mi) is set to1).

DC Link Capacitor

Mean DC output voltage of an IGBT-based chopper switch can be used to estimate its rating. Using a DC link capacitor, the output voltage of a rectifier is smoothed out, making it easier for the chopper switch to get a steady DC supply. An interruption in the waveform could affect the switch's ability to function. When the controller is turned on and off quickly, it creates a temporary short circuit. Thus, a danger of damage to the bridge rectifier is present in this case one explanation for this is that the charging current and ripple content can be significantly reduced using a trade-off voltage [11].

Fuzzy Logic Control

Because it relies on membership functions with values ranging from 0 to 1, fuzzy logic may handle situations with solutions that are vague or imprecise. Between membership and non-membership functions, there is a transition in fuzzy set theory.

Fuzzification, knowledge base, interference mechanisms, and defuzzification are the four key components of FLC. FLC's precise architecture is shown schematically in Figure 3.

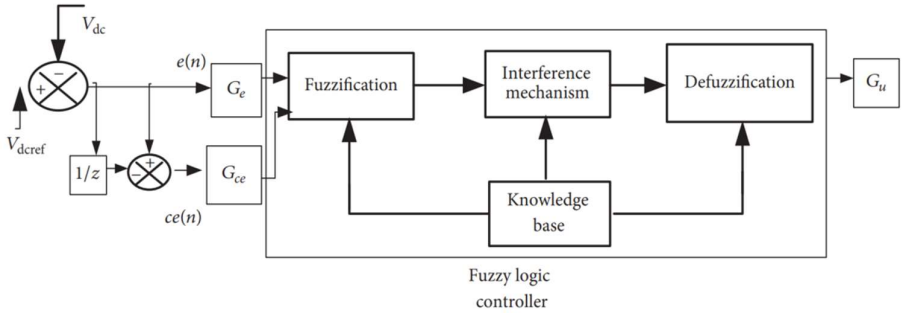

Figure 5: In-depth description of the fuzzy logic controller's structure.

The FLC's main inputs are DC voltage error and change. The fuzzy linguistic variables' membership functions are used to turn the input signals into fuzzy values through the fuzzification component. To produce fuzzified output, the interference mechanism applies a set of control rules and fuzzy information to input signals. Input circumstances are transformed into control signals using defuzzification methods such as centre of gravity and maximum, weighted mean, and so on. Using a triangle membership function, this fuzzy controller has a symmetrical characteristic along the central axis, making it straightforward to construct. The sampling error and the change in sampling error are primarily input into FLC.

$$e = V_{dcref} - V_{dc}$$

$$ce_n = e_n - e_{n-1}$$

An implied fuzzy set of tuning rules is obtained using Mamdani's maximin inference approach in this study. In the end, the indicated control signals are defuzzied using the centroid approach [14–16].

IV. ANN CONTROLLER FOR STATCOM

It is a mathematical model that consists of a number of simple pieces that work together. Training an ANN for a certain job is possible by adjusting the weights of the connections between the elements [10]. Scalar weight w_j multiplies with scalar weight p_i to get the product of the two scalars. All of the weights are added together to get $\sum wp_{ij}$, which is the sum of all the weights multiplied by the bias input. The weights and bias of the NN can be adjusted to achieve the desired result [10].

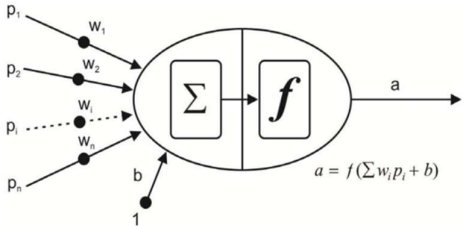

Fig 6. ANN $\sum wp_{ij}$.

MATHEMATICALANALYSIS OF ARTIFICIALNEURAL NETWORK

Neural network architectures come in a variety of forms. Two prominent ANN models are multi-layer perception (MLP) and radial bias function (RBF). The input, hidden, and output layers make up an MLP's three

main components. There is a neuron in figure 5, which is indicated by the suffix-i (see below). Input neurons are summated in g, which is an activation function.

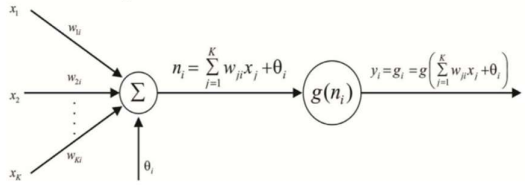

Fig-7 Single node in a Multi-Layer Perceptron network

Output of the ith neuron

$$U_i = g_i = g[\sum_{j=1}^{k} w_{ij}\, x_j + \theta_j]$$

The feed forward neural network is composed of layers, each of which serves a specific purpose. An iterative gradient algorithm is utilised as a training approach to reduce the mean square error between the reference signal and the actual signal.There are two types of j_{th} hidden layers, y_{net-j} and y_{out-j}, both of which include the suffix "j." The input and output layers are referred to as Unet and Uout, respectively, in computer terminology [11].

$$y_{net-j} = \sum_{i=1}^{n} w_{zi}\, x_i$$

$$y_{out} \quad = g(y_{net-j})$$

Where i=1,2,3…....n.

$$U_{net=\sum_{i=1}^{n} w_{yi} y_{out-j}} U_{out} = g(U_{net})$$

Where i=1,2,3,…….n.

$$w_{zi} = w_{zi.j} + \Delta w_{zi.j}$$

$$w_{yi} = w_{yi} + \Delta w_{zi}$$

$$g_x = \frac{2}{1 + e^{-x}} - 1$$

$w_{zi.j}$weights between the neurons of input layer and hidden layer.

$\Delta w_{zi.j}$ weight of ith input layer neuron to the jth hidden layer neuron.

NEURAL NETWORK TRAININGALGORITHM

Levenberg-Marquardt Use the BPA algorithm, Quasi-newton or the Levenberg-Marquardt method to do this task. The network's error can be decreased by using the network's output as a reference. The most exact results can be obtained by using this technique. This procedure defines the global error E value as [16-17].

$$E = \frac{1}{2}\sum (t_j - y_i)^2$$

Where y_i is the actual output andt_j is the desired outcome. y_i is the actual output. This approach combines the Gauss-Newton algorithm with the steepest descent method. This can be depicted as a weight increase [17].

$$w_{yi} = -\mu.\frac{UE}{UW_{yi}}$$

Updated weights between input neurons and the hidden layer [17] are updated.

$$\Delta w_{zi.j} = -\mu.\frac{UE}{UW_{zi,j}}$$

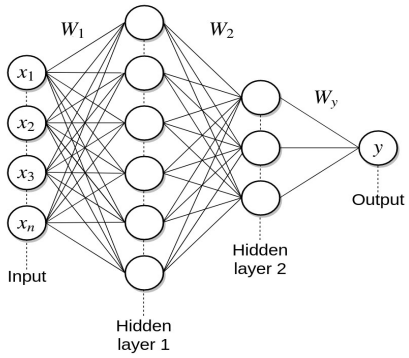

Fig8. ANN architecture

V.RESULTS

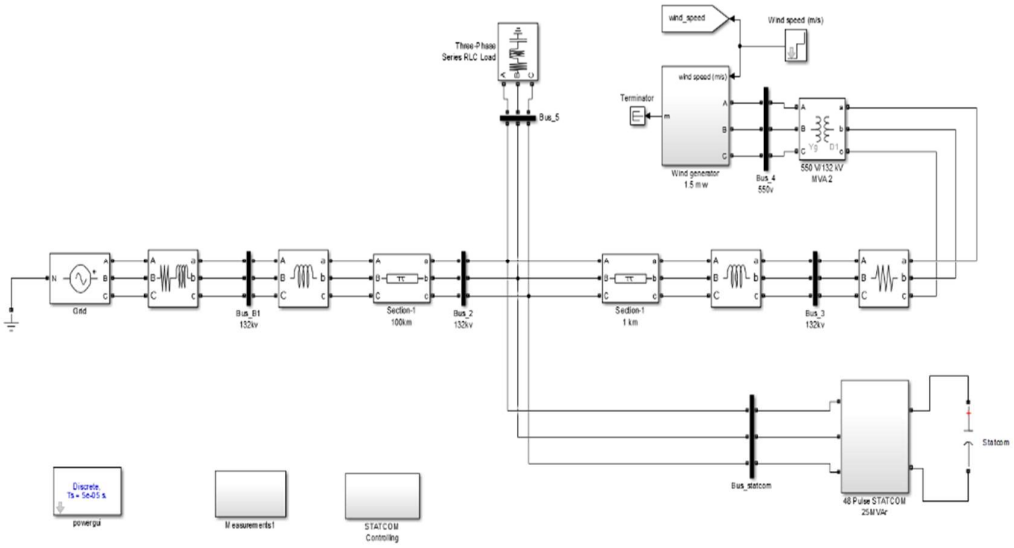

Fig 9. Simulation model diagram of the Proposed system.

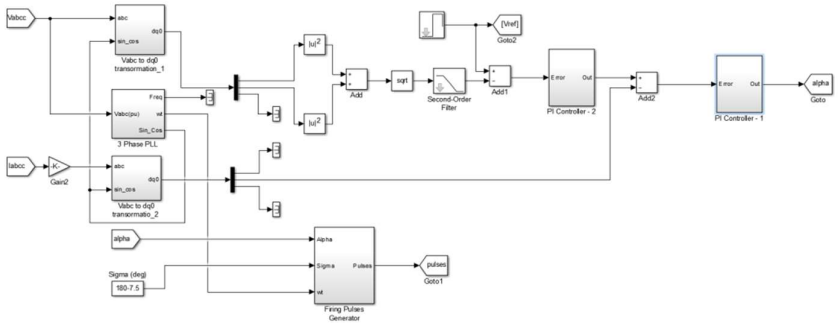

Fig10. Controller diagram with PI controller

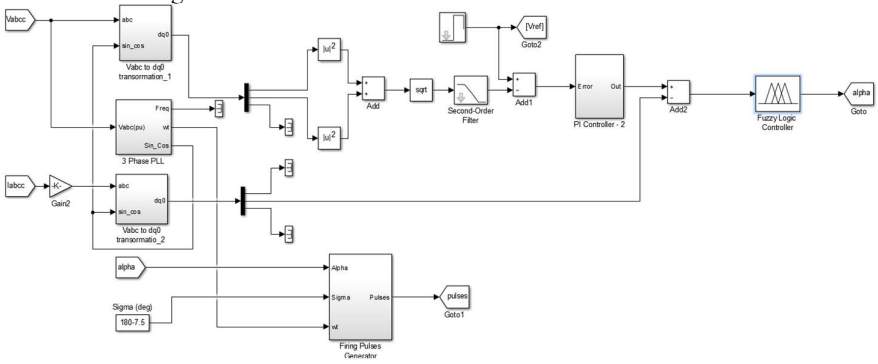

Fig11. Controller diagram with Fuzzy controller

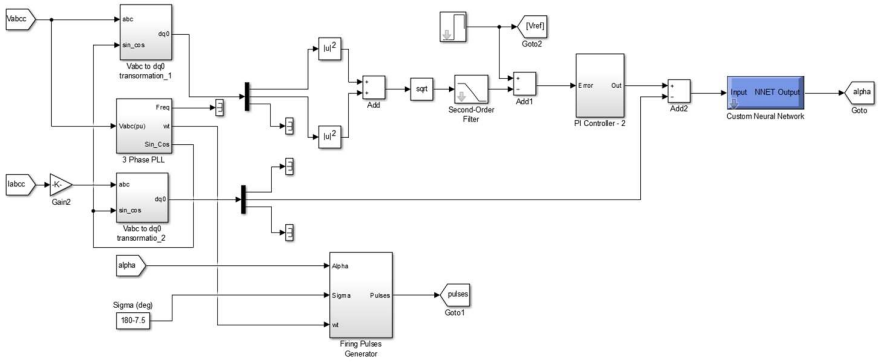

Fig12. Controller diagram with ANN controller

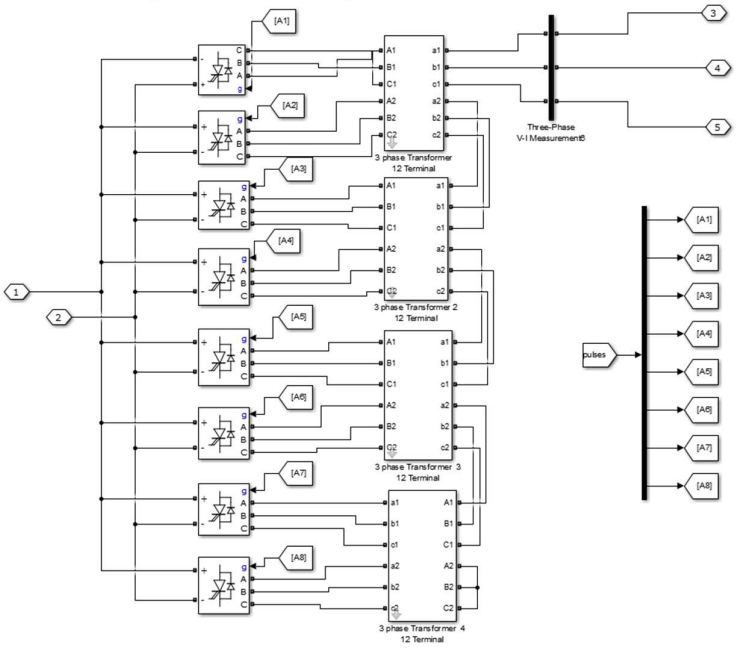

Fig13. 48 Pulse STATCOM device

.

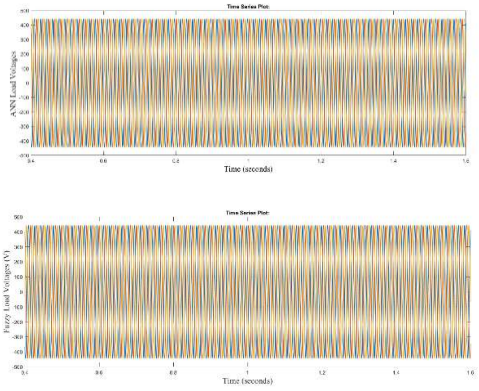

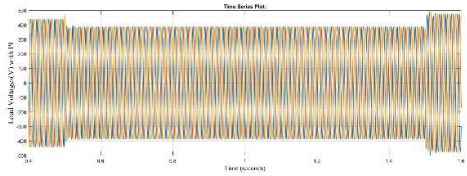

Fig14. Load Voltages (A) a) ANN b) Fuzzy c) PI

Above figure shows that the Load Voltages of the SEIG with 48 pulse STATCOM operates with the different controllers PI, Fuzzy and ANN. The Voltages are optimally controlled with the ANN and Fuzzy both the controllers give better results, and the THD of the system are controlled with the ANN when compared to the Fuzzy. In the system source voltages have a sag at the time period t= 0.5 with 380V and swell at the time t=1.5 with 420V. In the PI controller it is clearly exposed but in the fuzzy and ANN it was controlled.

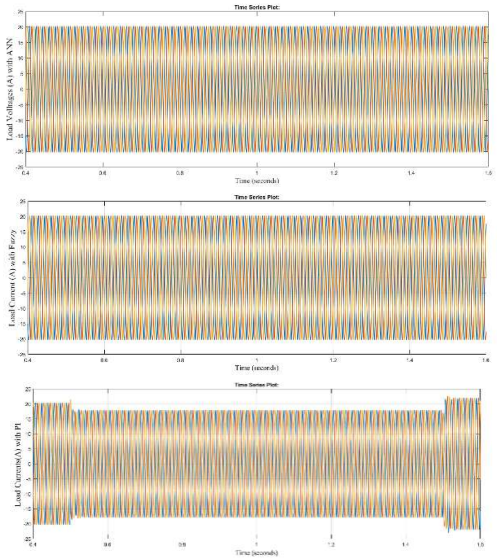

Fig15. Load Currents (A) a) ANN b) Fuzzy c) PI

In this project system source currents have a sag at the time period t= 0.5 with 18A and swell at the time t=1.5 with 22A. Above figure shows that the Load currents of the SEIG with 48 pulse STATCOM operates with the different controllers PI, Fuzzy and ANN. The currents are optimally controlled with the ANN and Fuzzy both the controllers give better results, and the THD of the system are controlled with the ANN when compared to the Fuzzy.

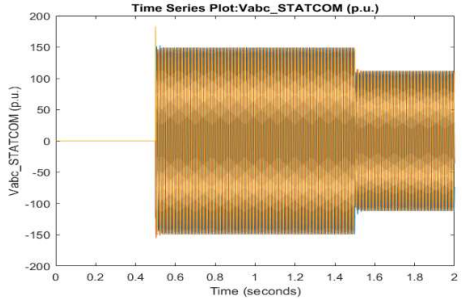

(a)

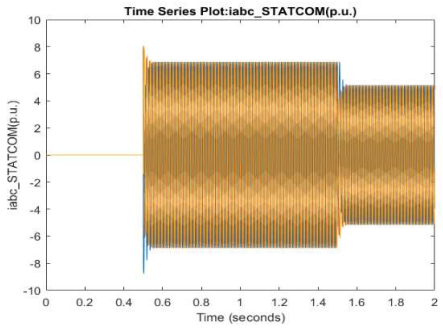

(b)

Fig16. STATCOM Voltages and Currents.

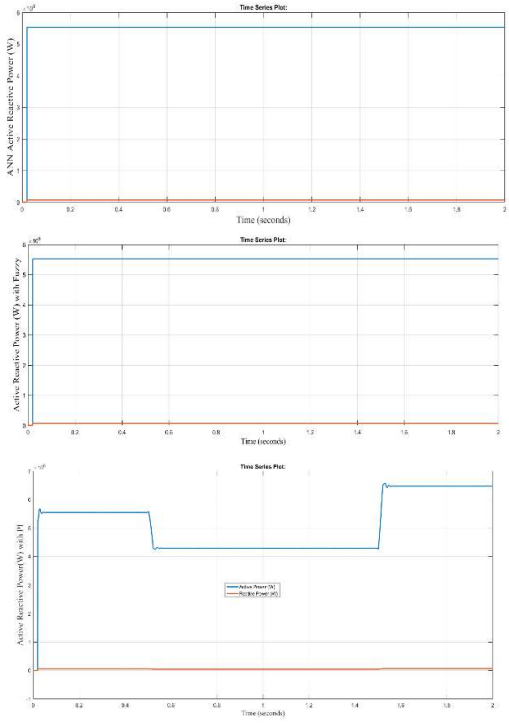

Fig17. Load Active Power Reactive power (A) a) ANN b) Fuzzy c) PI

Above figure shows that the Load Active Reactive power of the SEIG with 48 pulse STATCOM operates with the different controllers PI, Fuzzy and ANN. The Voltages are optimally controlled with the ANN and Fuzzy both the controllers give better results, and the THD of the system are controlled with the ANN when compared to the Fuzzy. In the system load Active Reactive power have a deviation at the time period t= 0.5 with 4.5MW and another deviation at the time t=1.5 with 6.5MW. In the PI controller it is clearly exposed but in the fuzzy and ANN it was controlled.

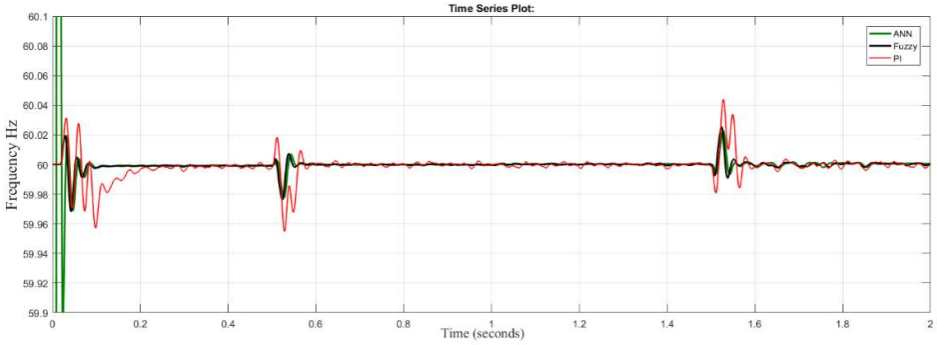

Fig18. Dynamic response of the Load frequency with PI, Fuzzy and ANN controllers

.

In the above figure the dynamic response of the Load frequency was shown as the results at the time t=0.1s, 0.5s and 1.5s there are slight deviations in the system PI and Fuzzy has more deviations compared to the ANN. And ANN performs better in the dynamic response of the SEIG system.

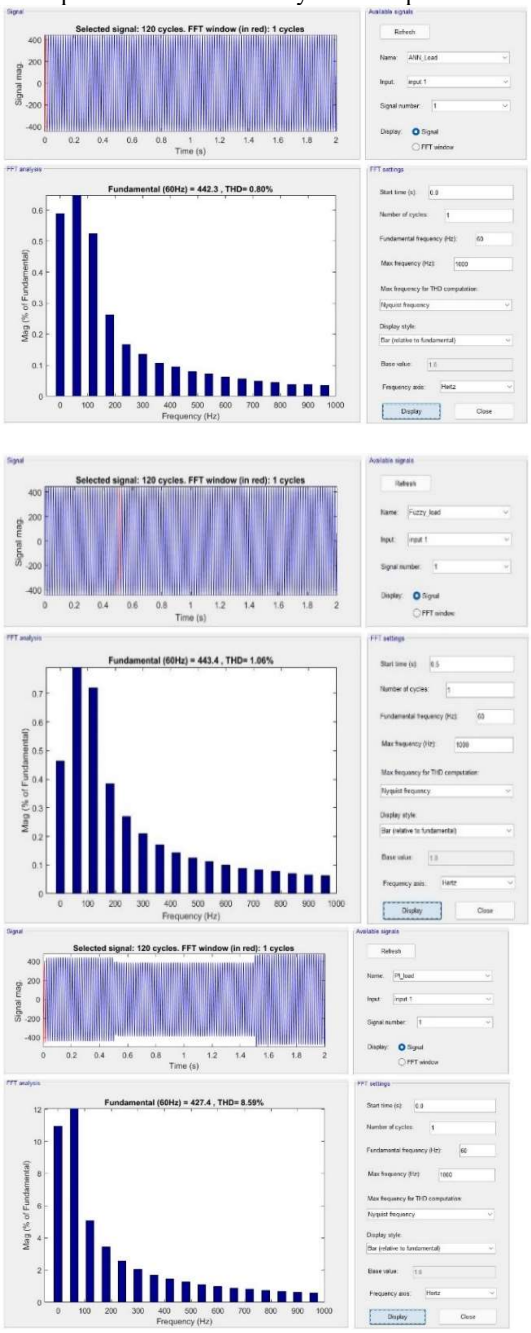

Fig19. FFT analysis of the Load Voltages a) ANN b) Fuzzy c) PI

Above figure shows the FFT analysis of the Load Voltages with the PI, Fuzzy and ANN controllers. Here, in the PI controller the Load voltages are with 8.6%, in fuzzy 1.06% and in the ANN 0.8% THD. ANN has a good response in controlling the THD of the System.

Table I

Controller Performances

Controller	**Controlling of THD%**	**Frequency**
PI	8.6%	59.89

Fuzzy	1.06%	59.94
ANN	0.8%	59.9

Conclusion

The self-excited operation of the induction generator is studied using a simulation. The variable terminal voltage and frequency of an uncontrolled SEIG renders it unsuitable for a wide range of applications. An induction machine needs to be modelled with a stationary reference frame for dynamic analysis. Magnetizing inductance is a critical consideration in voltage buildup. The SEIG's dynamic performance is provided by a wind turbine. In the Synchronous Reference frame, the flux is lined up with the D-axis. The d-q axis is decoupled by constructing a voltage decoupler. The q-axis current of the induction generator is used as a boost converter to regulate voltage. Wind turbine energy may be converted to grid electricity with a unity power factor by using a voltage source inverter. The new, more efficient technique is being used by the current controllers. This pulse generates both active and reactive power. In response to load and source side variations, the addition of new controllers to the outer loop improves ripple-free regulation of voltage and current. THD (total harmonic distortion) and dynamic responsiveness (DR) are some of the metrics used to gauge how effectively the controller works under various operating situations. For PI, Fuzzy, and ANN controllers, simulations in MatLab/Simulink are used to assess performance and active reactive power adjustment. In terms of performance, ANN beats out fuzzy and the PI controller.

REFERENCES

[1]B. Singh. "STATCOM-Based Voltage Regulator for Self-Excited Induction Generator Feeding Nonlinear Loads" , IEEE Transactions on Industrial Electronics, 10/2006.

[2] T. Anil Kumar, L. Shanmukha Rao. "Improvement of power quality of distribution system using ANN-LMBNN based DSTATCOM" , 2017 Innovations in Power and Advanced Computing Technologies (i-PACT), 2017

[3] Eshani Mishra, Sachin Tiwari. "Fuzzy logic control based Electronic Load Controller for Self-Excited Induction Generator" , 2016 International Conference on Electrical Power and Energy Systems (ICEPES), 2016.

[4] Mohamed I. Mosaad. "Model reference adaptive control of STATCOM for grid integration of wind energy systems" , IET Electric Power Applications, 2018.

[5] Bhim Singh, S. S. Murthy, Sushma Gupta. "Modelling of STATCOM Based Voltage Regulator for Self-Excited Induction Generator with Dynamic Loads" , 2006 International Conference on Power Electronic, Drives and Energy Systems, 2006.

[6] Mohamed I. Mosaad, Haitham Saad Mohamed Ramadan, Mansour Aljohani, Mohamed F. El-Naggar, Sherif S. M. Ghoneim. "Near-Optimal PI Controllers of STATCOM for Efficient Hybrid Renewable Power System" , IEEE Access, 2021.

[7] Bhim Singh, Gaurav Kumar Kasal, Ambrish Chandra, Kamal-Al-Haddad. "A frequency based electronic load controller for an isolated asynchronous generator feeding 3- phase 4-wire loads" , 2008 IEEE International Symposium on Industrial Electronics, 2008.

[8] Bhim Singh, Gaurav Kumar Kasal. "Adaline Based Control of Solid-State Voltage Regulator for Isolated Asynchronous Generators" , 2006 International Conference on Power Electronic, Drives and Energy Systems, 2006

[9] Chetana, Gaound, S K Shah, and S J Patel. "Analysis and design of electronic load controller using FLC for self-excited induction generator" , 2012 1st International Conference on Emerging Technology Trends in Electronics Communication & Networking, 2012.

[10] B. Singh, S.S. Murthy, S. Gupta. "A Stand-Alone Generating System Using Self-Excited Induction Generators in the Extraction of Petroleum Products" , IEEE Transactions on Industry Applications, 2010

[11] P. K. Singh, Y. K. Chauhan. "Performance analysis of multi-pulse electronic load controllers for self-excited induction generator" , 2013 International Conference on Energy Efficient Technologies for Sustainability, 2013

[12] Singh, Bhim, and V Rajagopal. "Integrated solid-state controller for small hydro generation using isolated asynchronous generator" , 2010 International Conference on Power Control and Embedded Systems, 2010.

[13] Yasin Seker, Evren Dilek Şengür. "The Impact of Environmental, Social, and Governance (ESG) Performance on Financial Reporting Quality: International Evidence" , Ekonomika, 2021

[14] "STATCOM-Based Controller for a ThreePhase SEIG Feeding Single-Phase Loads" , IEEE Transactions on Energy Conversion, 2014

[15] R.S. Bhatia, S.P. Jain, Dinesh Kumar Jain, B. Singh. "Battery Energy Storage System for Power Conditioning of Renewable Energy Sources" , 2005 International Conference on Power Electronics and Drives Systems, 2005

[16] Sergey I. Tarasov. "Phylogenetic analyses reveal reliable morphological markers to classify mega-diversity in Onthophagini dung beetles (Coleoptera: Scarabaeidae: Scarabaeinae)" , Cladistics, 10/2011

[17] Celestina Cotti Ferrero, Giovanni Ferrero. "Chapter 4 Multiplicative Identities and Commutativity Conditions" , Springer Science and Business Media LLC, 2002

[18] Saber Mohamed Saleh Salem. "Study of wind turbine based self-excited induction generator under nonlinear resistive loads as a step to solve the Egypt electricity crisis" , Computers & Electrical Engineering, 2016.